SoRX: A Soft Pneumatic Hexapedal Robot to Traverse Rough, Steep, and Unstable Terrain

Zhichao Liu, Zhouyu Lu, and Konstantinos Karydis

***Abstract*— Soft robotics technology creates new ways for legged robots to interact with and adapt to their environment. In this paper we develop i) a new 2-degree-of-freedom soft pneumatic actuator, and ii) a novel soft robotic hexapedal robot called SoRX that leverages the new actuators. Simulation and physical testing confirm that the proposed actuator can generate cyclic foot trajectories that are appropriate for legged locomotion. Consistent with other hexapedal robots (and animals), SoRX employs an alternating tripod gait to propel itself forward. Experiments reveal that SoRX can reach forward speeds of up to 0.44 body lengths per second, or equivalently 101 mm/s. With a size of 230 mm length, 140 mm width and 100 mm height, and weight of 650 grams, SoRX is among the fastest tethered soft pneumatically-actuated legged robots to date. The motion capabilities of SoRX are evaluated through five experiments: running, step climbing, and traversing rough terrain, steep terrain, and unstable terrain. Experimental results show that SoRX is able to operate over challenging terrains in open-loop control and by following the same alternating tripod gait across all experimental cases.**

I. Introduction

Multi-legged robots show promise in application areas such as search-and-rescue and intelligence-surveillance-reconnaissance (ISR) where operation over rough and unstructured terrain is expected. However, achieving all-terrain mobility remains a challenging task, especially as robots scale down in size [1].

Adaptation to terrain variations is key for taking the robots outside of the protected laboratory environment, and deploying them in real-world settings. Studies have indicated that incorporating compliant legs, as animals do, can significantly improve the speed and stability of these robots in varying environmental conditions [2]. Among the first efforts to incorporate passive mechanical compliance within a robot's legs was the springy C-leg in the hexapedal robot RHex [3]–[5], which is still commonly used nowadays. Tunable devices were proposed to adjust the stiffness of legs [6]–[8]. Direct-drive legged robots were also developed to achieve variable compliance (e.g., [9]–[12]).

There have been other attempts to achieve tunable stiffness using antagonistic pneumatic actuators such as McKibben actuators and pleated pneumatic artificial muscles [13], [14]. However, these compliant legs come together with rigid parts, which limit the contact area along the length of legs, therefore reducing the ability to navigate rough terrain.

Fig. 1: SoRX, the novel soft legged robot developed in this work. The robot is able to traverse terrains consisting of sand and rocks.

Soft robotics is a relatively young field, with challenges in design, fabrication and control [15]. Soft robots are particularly appropriate for locomotion in uneven and/or sensitive environment, because their soft structure allows them to bend and squeeze to fit their shape around obstacles, and reduce the stress induced by contact over both surroundings and the robots surface [16]. In particular, soft robotics have been investigated and developed for locomotion applications. Prior work includes soft robots powered by soft pneumatic actuators (SPA) to achieve crawling and undulation gaits [17]–[19]. A starfish-like soft robot was developed to complete crawling gaits actuated by shape memory alloys [20]. However, the actuators of these robots only have only one degree of freedom (DoF). Meanwhile, they are unable to traverse over rough terrain as more rigid legged robots do. Notable exceptions include a robot that combines soft legs with wheels for navigation on uneven terrain [21], and a soft-material 3D-printed pneumatic legged robot able to lift its legs off the ground and walk over unstructured terrain [22]. Nevertheless, these robots rely on either rigid wheels or multiple leg configurations to achieve all-terrain locomotion. Moreover, unlike hexapedal robots, they cannot sustain a large support area, as with an alternating tripod gaits, which can be advantageous when traversing uneven terrain [23].

There are other attempts to achieve soft legged locomotion by leveraging cable-driven actuators. The Sofia walking robot [24] and Puppy [25] utilize model-based optimal control to achieve walking locomotion. The cable-driven legs have 2 DOFs: bending and extension. Compared to pneumatic ones, cable-driven actuators may be more direct to model and control. However, cable-driven actuators can be

The authors are with the Dept. of Electrical and Computer Engineering, University of California, Riverside. Email: {zliu157, zlu044, karydis}@ucr.edu.

We gratefully acknowledge the support of NSF under grant # IIS-1910087 and of the UCR Office of Research and Economic Development under a Collaborative Seed Grant. Any opinions, findings, and conclusions or recommendations expressed in this material are those of the authors and do not necessarily reflect the views of the funding agencies.

challenged when it comes to varying leg stiffness to adapt to terrain variations. Moreover, the necessary motors may render cable-driven robots top-heavy and thus unstable [25].

In this paper we present a new soft pneumatic actuator with 2 DoFs. We use Finite Element Analysis to predict its performance and expected motion in simulation. Equipped with a pressurizing/depressurizing air control board, we evaluate experimentally the bending and extension capacity of physical actuator prototypes, identify a pressurization/depressurization sequence to generate appropriate cyclic foot trajectory profiles, and confirm that the proposed actuators can be used as legs for a pneumatically-actuated soft robot. Leveraging the new actuators, we design and manufacture a tethered soft legged robot prototype, the Soft Robotic heXapod (SoRX) shown in Fig. 1. To the best of our knowledge, SoRX is the fastest soft pneumatic legged robot to date. More importantly, it is the first soft pneumatic legged robot able to operate over a range of challenging environments, such as rough, steep, and unstable terrain, without any additional control effort and by following the same alternating tripod gait across all terrains.

Succinctly, our contributions are as follows:

- We develop a new soft pneumatic actuator with 2 DoFs, and evaluate its performance both in simulation and physical testing.
- We design and manufacture a tethered soft pneumatic hexapedal robot and analyze its gait.
- We investigate the robot's motion capabilities on locomoting over rough, steep and unstable terrain.

II. Soft Leg Design, Fabrication, and Analysis

A. A Soft Pneumatic Actuator Leg Design

To design an all-terrain soft legged robot, each leg must be sufficiently compliant to adapt to obstacles, while stiff enough to support the robot's weight. One promising way to balance this trade-off is by utilizing soft pneumatic actuators (SPAs). Prior works on SPAs for legged locomotion have relied on pneumatic networks (PneuNets) [17] and multiple bellowed chambers [22]. However, these actuators can only bend but not extend, which may constrain the locomotion capabilities of the robot in practice.

To mitigate this challenge, we introduce the SPA design shown in Fig. 2. The actuator consists of two parts: 1) the bending part, which is adopted by the original PneuNet design with one cut remaining, and 2) the extension part, which employs a Hyper-Elastic Bellows (HEB) actuator design [26]. When the two parts are pressurized, the actuator can both bend and extend; different pressurization/depressurization cycles can then yield a multitude of distinct foot trajectory profiles (more on this later in Section III).

B. Fabrication

Each actuator is cast separately out of two-part silicone elastomer (Dragon Skin 10 FAST, Smooth-On). Three pairs of 3D-printed molds (Onyx material on Markforged Mark Two carbon fiber 3D printer) are used to form shapes (Fig. 3). The bending part consists of two pieces: the chamber and

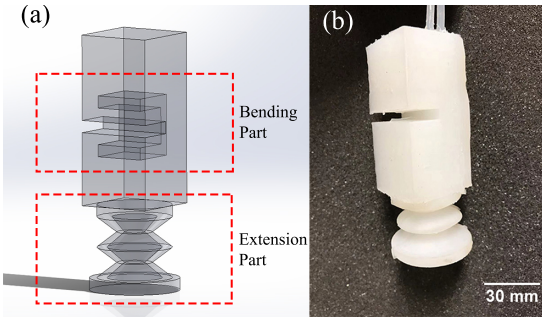

Fig. 2: (a) CAD rendering, and (b) a physical actuator prototype.

button layer, which are molded separately. Overall, fabrication of a leg takes place in four steps. 1) Mix the elastomer and process it in vacuum chamber to remove bubbles. 2) Pour it into the molds and wait 75 minutes for it to cure, and demold the pieces. 3) Use an adhesive (Sil-Poxy, Smooth-On) to bond together the two pieces of the bending part. Meanwhile, glue two same silicone bodies made by mold (c) in Fig. 3 to form the extension part. 4) Insert silicone tubes for air connection and bond the two actuator parts.

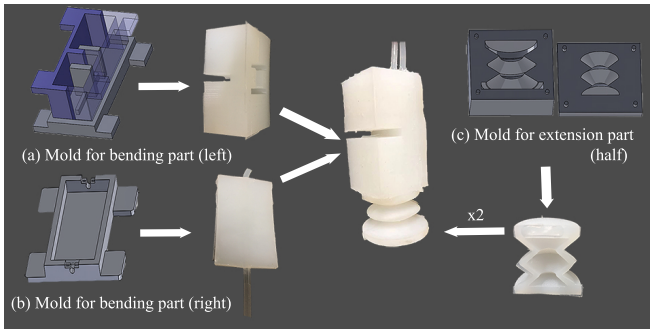

Fig. 3: Fabrication of the soft pneumatic actuator

C. Simulated Actuator Behavior

Simulation was conducted to guide the design and to ensure the proposed design can work as intended in real-time. We used Finite Element Method (FEM) analysis to simulate large non-linear deformations undergone by soft structures, by following the analysis in [27]. In sum, at each step i of the real-time simulation, the internal forces are linearized as

$$f(x_i) \approx f(x_{i-1}) + K(x_{i-1})dx \ , \tag{1}$$

where f is the volumetric internal stiffness force at the nodes, and $K(x)$ represents the tangent stiffness matrix. Assuming quasi-static motions, the model is in equilibrium in terms of internal and external forces, that is

$$-K(x_{i-1})dx = p + f(x_{i-1}) + J^T\lambda \ , \tag{2}$$

where p stands for the external forces, λ represents the contributions of the actuators and the contact forces (if applicable) and J gathers the directions [27].

To solve for node displacements, we first find a free configuration x^{free} by solving (2) with $\lambda = 0$. The result also yields δ^{free} which is the violation for constraints. Then,

a constraint-based solver computes λ given laws of the constraint between δ and λ, that is

$$\delta = \underbrace{\left[JK^{-1}J^{T}\right]}_{W}\lambda + \delta^{\text{free}} \ . \tag{3}$$

Finally, node displacements are calculated using the value of the constraint response [27]

$$x_t = x^{\text{free}} + K^{-1}J^{T}\lambda \ . \tag{4}$$

All steps are implemented in SOFA [28][1] with SoftRobot-Plugin [29].[2] The mesh file consists of $13,344$ tetrahedra and $3,352$ nodes. To build a precise simulation, elastic and inertial parameters have to be tuned in simulation. The Young's modulus is obtained from silicone's properties while the mass of the actuator is measured experimentally [30]. Figure 4 shows simulation results when the actuator is pressurized and depressurized. Comparisons between trajectories in simulation and in physical testing are given in Section III.

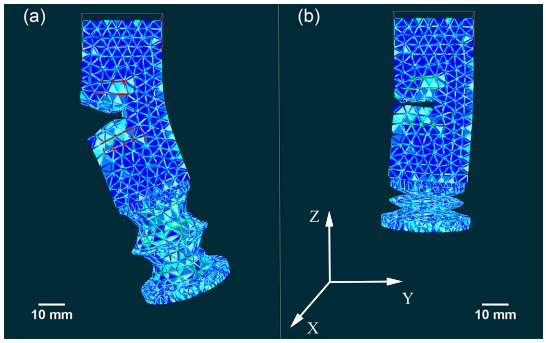

Fig. 4: FEM analysis of leg (a) pressurization and (b) depressurization in the SOFA environment. Each tetrahedron represents the FEM force field. Node displacements demonstrate changes in shape.

D. Actuator Performance

The actuator's properties regarding extension, bending, and stiffness-varying have a significant impact on its utility to soft legged robots. To this end, we conducted empirical tests to validate simulation results, and to evaluate the performance of the physical prototype.

In the extension and bending tests, the actuator was mounted horizontally (see Fig. 5). Both extension and bending parts are pressurized/depressurized at 2.5 kPa increments. The position of the actuator's free end was recorded in the extension test. In simulation, the direction of gravity points to the negative direction along Y-axis to match the experimental setting (see Fig. 4). To represent the additional rigidity created by the silicone tube in the bending part, we used a model of stiff springs in the direction of the tubes [31]. We exported the position of the corresponding node via a Python script in SOFA. Extension test results (Fig. 5) show the experimentally-measured values match the simulation data. The extension part can elongate by 48 mm at 30 kPa and be shortened by 9 mm in depressurization. It is worth mentioning that the simulation diverged when pressure values extended beyond the range of $[-2, 10]$ kPa.

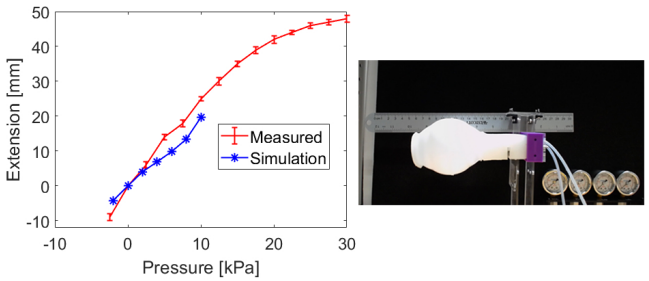

Fig. 5: Results and experimental setup for the extension test. Negative pressure numbers relate to depressurization (vacuum) mode of the air source.

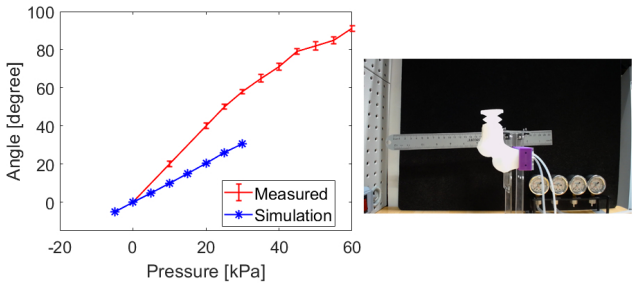

Fig. 6: Results and experimental setup for the bending test.

In the bending test we measured bending angles as input pressure varies. Results (Fig. 6) show that the actuator can bend 91 deg at 60 kPa. However, angles in simulation are smaller than the measured ones. Further, simulations diverged when the input pressure exceeded 30 kPa.

In both tests, we observed some mismatch between the measured and simulated results. This mismatch may be caused by approximations in material properties such as Young's modulus and Poisson ratio,[3] measurement errors, and vibrations caused while the actuator was pressurized.

Moreover, we measured the force generated by the actuator as a function of the input pressure to illustrate the actuator's stiffness-varying property. In this test, the actuator was mounted vertically above a load cell with amplifier HX711 and microcontroller Arduino Mega (Fig. 7). The actuator was in contact with the load cell when the pump was switched off. Input pressure values ranged from 0 kPa to 20 kPa. Results indicate that the actuator can apply 10.67 N at 20 kPa. As such, our hexapedal robot can lift a maximum weight of 3.26 kg when it follows an alternating tripod gait.[4] Note that the bending part was not actuated in this test. However, as pressure increases over a critical point, the leg will passively bend; this effect can lead to the sharp increase observed in Fig. 7 at approximately 13 kPa.

III. SoRX Design and Gait Analysis

The new soft actuators are used to create the pneumatically-actuated soft robotic hexapod SoRX (Fig. 1, and Fig. 8). SoRX measures 230 mm L $\times$ 140 mm W $\times$

[1] https://www.sofa-framework.org/

[2] https://project.inria.fr/softrobot/

[3] Material properties may vary due to fabrication, e.g., it is very difficult to remove all air bubbles during casting despite using a degassing chamber.

[4] That is, three legs are touching the ground at all times.

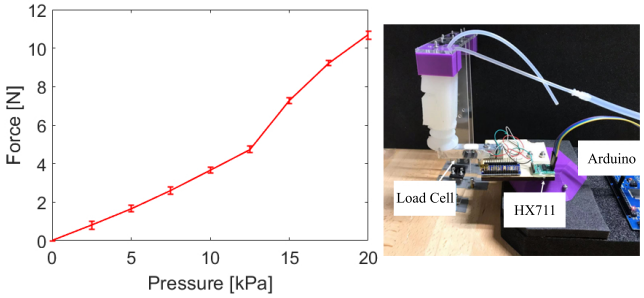

Fig. 7: Results and experimental setup for the stiffness-varying test.

100 mm H and weighs 650 g. The frame of SoRX was manufactured by combining laser-cut wood and acrylic sheets (Universal Laser Systems VLS 3.60 laser cutter), and six 3D-printed leg holders (Makerbot Replicator+ 3D printer).

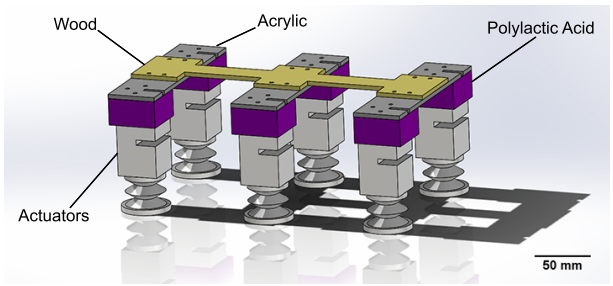

Fig. 8: CAD of SoRX and materials.

A. Gait Analysis

Like RHex [32] and DASH [33], among other hexapods, SoRX employs an alternating tripod gait for locomotion. Static stability is guaranteed with alternating tripods by keeping the center of mass within the support area formed by the three legs that touch the ground.

To achieve effective locomotion we need to determine appropriate cyclic control trajectories for the robot's feet. However, determining pressurization/depressurization sequences for pneumatically-actuated soft legged robots is a challenging task. As shown shortly, available simulation tools yield quite different results from those observed in practice. In this work, we identified empirically a pressurization/depressurization sequence that can lead to effective locomotion. The sequence is shown in Fig. 9(a). Bending and extension parts are pressurized sequentially, and then they are depressurized simultaneously. Temporal duration ratios remain fixed; changing the total cycle time leads to different forward velocities.

To identify the nominal foot trajectory, the actuator was mounted vertically as in the stiffness-varying test. The vertical axis points to the opposite direction of gravity, thus the vertical displacements are negative. An entire actuation sequence was applied to the actuator while the camera recorded motion. Resulting image frames were post-processed and analyzed with the video analysis software Kinovea. Meanwhile, the same actuation sequence was applied in simulation. Resulting trajectories are shown in Fig. 9(b). We notice that the foot returns to its original starting point after one stride despite the very compliant nature of the leg. A maximum foot clearance of about 14 mm was recorded. Device vibrations may cause non-smooth points in the trajectory. Further, we noticed that the bending part tended to respond faster to differential pressure inputs than the extension part. The last two points are the major differences between simulation and experiment (i.e. trajectories are smoother, and actuators respond equally fast in simulation). These differences may be caused by the various approximations noted previously in Section II-D, but also by the fact that the simulation relies on the assumption of quasi-static motions, which is not met in rapid actuation cycles needed in practice.

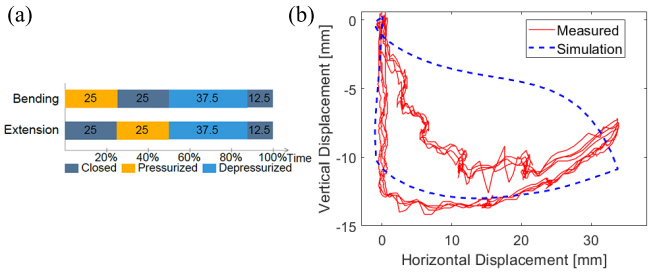

Fig. 9: (a) Empirically-derived actuation sequence for one leg stride. (b) Resulting simulated (in blue) and experimental (in red) foot trajectories.

IV. Experiments and Results

The motion capabilities of SoRX were evaluated through five experiments: running, step climbing, and traversing rough terrain, steep terrain, and unstable terrain. A modified version of an open-source pneumatic control board [34] was used in all experiments. In our board, every air output channel is connected to two pairs of valves and pumps to allow for both pressurization and depressurization. The primary experimental testbed is shown in Fig. 10. At this stage the robot runs in open loop (i.e. without steering control); hence, two acrylic panels were used to ensure the robot does not fall off from the platform. The length of the platform is 1.2 m. A 12-camera VICON motion capture system was used to collect position and velocity data of the center-of-mass (CoM) of SoRX.

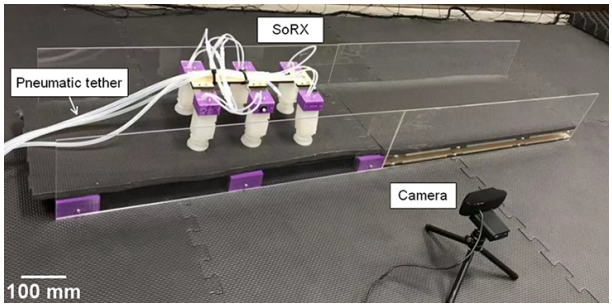

Fig. 10: Primary experimental testbed to evaluate performance in running, step climbing, and traversing rough terrain.

A. Running

SoRX was able to reach a top speed of 0.44 body lengths per second (BL/s), or 101 mm/s, at maximum actuation pressures of 34 kPa for the bending part and 10 kPa for the extension part. Figure 11 depicts an instance of the

robot running. Compared to other soft robots, SoRX can run significantly faster both in terms of body length and absolute distance (Table I). To the best of our knowledge, SoRX is the fastest to date pneumatically-actuated soft legged robot.

Fig. 11: Snapshots in 0.5 sec intervals of SoRX running.

TABLE I: Speeds for soft robots

Robots	Speed [BL/s]	Speed [mm/s]
SoRX	0.44	101.0
Quadrupedal [22]	0.14	20.0
Puppy [25]	0.12	15.6
Multigait [17]	0.05	6.7
Five-limb [20]	0.003	0.43

Further, we performed running tests at two distinct speeds set at 0.35 BL/s and 0.44 BL/s, to capture the evolution of the position of SoRX's CoM in forward motion. Results reveal that the robot's CoM follows a repeatable cyclic pattern (Fig. 12). This observation is consistent with the CoM evolution of more rigid legged robots, suggesting that related tools to study stability and to design motion planners and controllers may be appropriate for soft legged robots as well.

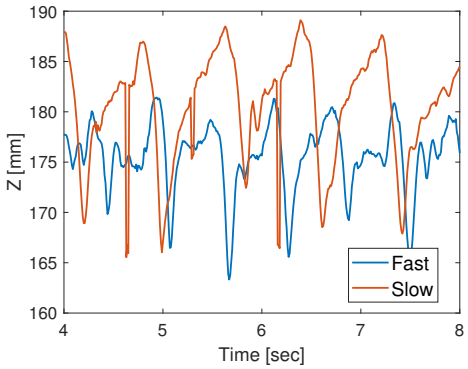

Fig. 12: CoM position evolution in the Z axis at two different forward speeds, 0.44 BL/s (in blue) and 0.35 BL/s (in red), indicating that the robot's CoM follows a cyclic pattern.

B. Step Climbing

SoRX was able to overcome obstacles up to 15 mm tall passively and while following the same alternating tripod gait used for running (Fig. 13). Leg softness appears to play a dual positive role. First, it can improve locomotion robustness by enabling SoRX to recover when one leg gets stuck on the obstacle. Second, it may help overcome obstacles larger than the nominal foot clearance. (Recall the nominal foot clearance was measured at 14 mm in static single-leg tests shown in Fig. 5.) In both cases, a leg may forcibly squeeze or over-extend beyond the range prescribed through its actuated values without any damage if forces remain below the silicone's yield point.

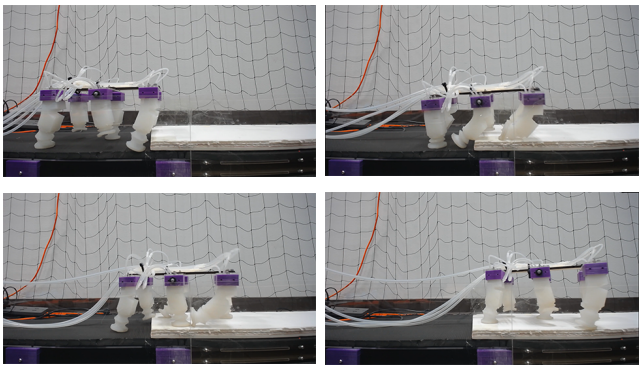

Fig. 13: SoRX climbing over a 15 mm-tall stack of foam board.

C. Traversing Rough Terrain

To evaluate the robot's capability to traverse rough terrain, we considered locomotion over sand, rocks, and a mixed terrain (Fig. 14). The mixed terrain consisted of two flat ground parts at the two ends, as well as sand and rocks parts in the middle. The supplementary video offers a clear illustration of our experiments.

The speed of SoRX while traversing rough terrain is compared to the speed of Quadrupedal [22]. Quadrupedal was tested with small pebbles and large rocks. Therefore, the speed of SoRX over sand is compared to the one of Quadrupedal over small pebbles. Results (shown in Fig. 15) demonstrate that SoRX is able to navigate much faster on all types of terrain. Unlike Quadrupedal, SoRX uses one leg configuration that is adequate for flat ground and rough terrain alike. The speed of SoRX over mixed terrain suggests that keeping the same gait pattern and control effort may suffice to traverse different types of terrain.

Fig. 14: SoRX was found capable to traverse (a) sand, (b) rocks, and (c) mixed terrain.

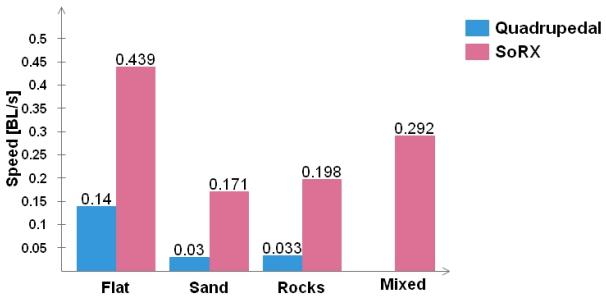

Fig. 15: Terrain traversal speeds for Quadrupedal and SoRX.

D. Traversing Steep Terrain

Walking over inclined surfaces has been a challenging task for all legged robots. A spherical soft robot [35] was able to

climb a slope with crawling gaits. Puppy [25] can walk up a hill only in simulation.

Two experiments were implemented to test SoRX's locomotive performance on steep terrain: 1) walking on an inclined flat surface, and 2) walking inside an inclined groove. The robot was able to climb up to a 10 deg angled flat surface made of acrylic sheet as shown in Fig. 16(a) while employing the same alternating tripod gait as in running over flat and rough terrain and climbing over a step. Moreover, the robot was able to traverse a 15 deg inclined groove made of two flat acrylic sheets as shown in Fig. 16(b). The actuators can bend and squeeze to fit the high-slop surface. Unlike Quadrupedal, SoRX does not require any additional leg configuration to handle steep terrain. The supplementary video shows more clearly how the robot performs in these challenging terrains.

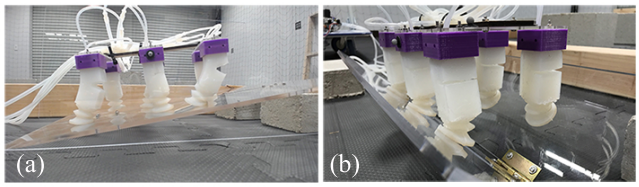

Fig. 16: (a) SoRX climbing up a slope of 10 deg. (b) SoRX shown inside an inclined groove where actuators bend and squeeze to adapt to the high-slope surface.

E. Traversing Unstable Terrain

To further evaluate the robustness of SoRX's running performance, we commanded SoRX to run on an unstable (oscillating) platform. The experimental setup consisted of four caster wheels supporting a wooden sheet; see Fig. 17(a). The platform oscillated in the X-Y plane while SoRX was running on top of it.

Figure 17(b) superimposes the speed of SoRX and of the oscillating platform's as measured through motion capture. SoRX was able to run on the platform without tipping over despite the platform oscillating at speeds comparable to the robot's forward velocity. The employed alternating tripod gait, paired with soft legs appear to yield a robust running performance in spite of the unstable (oscillating) terrain.

V. Conclusions

Pneumatically-actuated soft legged robots may serve as a new tool to applications where operation over rough and unstructured terrain is required, e.g., when looking for survivors in the aftermath of an earthquake. Operation in such terrains still challenges more rigid legged robots; instead, soft legged robots could squeeze and bend to overcome obstacles and fit into crevices to explore their environment.

In this paper, we presented SoRX, a novel pneumatically-actuated soft hexapedal robot. SoRX utilizes our new 2-DoF soft pneumatic actuators that can both bend and extend to create foot trajectory profiles that are appropriate for legged locomotion. Consistent with other hexapedal robots (and animals), SoRX employs an alternating tripod gait to propel itself forward. We showed that the alternating

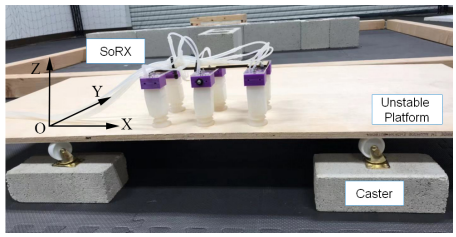

(a)

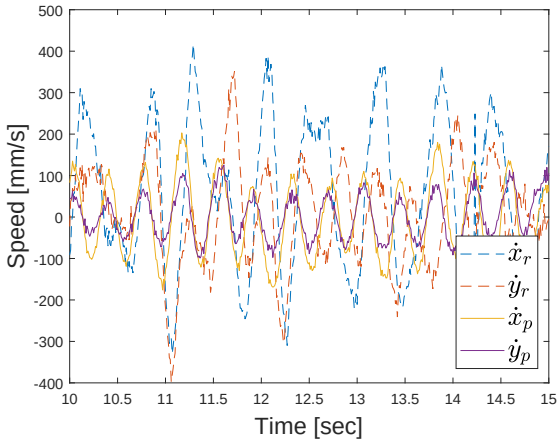

(b)

Fig. 17: (a) Experimental setup for the unstable terrain testing. Terrain is oscillating in the X-Y plane at speeds comparable to the robot's forward speed, topping at approximately 200 mm/s. (b) Superimposed platform (solid curves) and robot (dashed curves) speeds for the unstable terrain testing. $(\dot{x}_p, \dot{y}_p)$ and $(\dot{x}_r, \dot{y}_r)$ denote the platform and combined robot and platform speeds, respectively. (Figure best viewed in color.)

tripod gait can be utilized for effective locomotion of SoRX while traversing flat, rough, steep, and unstable (oscillating) terrains. Experiments reveal that SoRX can reach forward speeds of up to 0.44 BL/s, which to the authors' best of knowledge makes it the fastest soft pneumatically-actuated legged robot to date. The robot can climb over 15 mm tall obstacles, walk over terrains that contain rocks, sand, and combination of those, climb up to 10 deg slope, and walk inside 15 deg inclined grooves. SoRX is also capable to run on an unstable platform oscillating at speeds comparable to the robot's forward speed without tipping over. These results suggest that compliance introduced through a purely soft leg design may create new opportunities for legged robots to navigate over challenging terrains.

To realize the potential of soft legged robots in applications, several challenges remain to be addressed. Among them is to enable untethered operation while keeping the size and weight of the robot within reasonable limits. Our future work will seek to explore more motion capabilities, such as turning and moving backward. We will study the effect of different elastic modules and stiffness of the flexible legs on the moving performance. Furthermore, we plan to develop control strategies for trajectory tracking and enable SoRX to work autonomously, untethered, and with integrated sensing capabilities.

REFERENCES

[1] J. Z. Kolter, M. P. Rodgers, and A. Y. Ng, "A control architecture for quadruped locomotion over rough terrain," in *IEEE International Conference on Robotics and Automation (ICRA)*, 2008, pp. 811–818.

[2] J. Rummel, Y. Blum, H. M. Maus, C. Rode, and A. Seyfarth, "Stable and robust walking with compliant legs," in *IEEE International Conference on Robotics and Automation (ICRA)*, 2010, pp. 5250–5255.

[3] E. Moore, D. Campbell, F. Grimminger, and M. Buehler, "Reliable stair climbing in the simple hexapod 'rhex'," in *IEEE International Conference on Robotics and Automation (ICRA)*, vol. 3, 2002, pp. 2222 – 2227.

[4] R. Altendorfer, N. Moore, H. Komsuoglu, M. Buehler, H. Brown, D. McMordie, U. Saranli, R. Full, and D. E. Koditschek, "Rhex: A biologically inspired hexapod runner," *Autonomous Robots*, vol. 11, no. 3, pp. 207–213, 2001.

[5] U. Saranli, M. Buehler, and D. E. Koditschek, "Rhex: A simple and highly mobile hexapod robot," *The International Journal of Robotics Research*, vol. 20, no. 7, pp. 616–631, 2001.

[6] J. W. Hurst, J. E. Chestnutt, and A. A. Rizzi, "An actuator with physically variable stiffness for highly dynamic legged locomotion," in *IEEE International Conference on Robotics and Automation (ICRA)*, vol. 5, 2004, pp. 4662–4667.

[7] K. C. Galloway, J. E. Clark, and D. E. Koditschek, "Design of a tunable stiffness composite leg for dynamic locomotion," in *ASME International Design Engineering Technical Conferences and Computers and Information in Engineering Conference (IDETC/CIE)*, 2009, pp. 215–222.

[8] A. Enoch, A. Sutas, S. Nakaoka, and S. Vijayakumar, "Blue: A bipedal robot with variable stiffness and damping," in *IEEE-RAS International Conference on Humanoid Robots (Humanoids)*, 2012, pp. 487–494.

[9] G. Kenneally, A. De, and D. E. Koditschek, "Design principles for a family of direct-drive legged robots," *IEEE Robotics and Automation Letters*, vol. 1, no. 2, pp. 900–907, 2016.

[10] J. Hwangbo, J. Lee, A. Dosovitskiy, D. Bellicoso, V. Tsounis, V. Koltun, and M. Hutter, "Learning agile and dynamic motor skills for legged robots," *Science Robotics*, vol. 4, no. 26, 2019.

[11] T. Apgar, P. Clary, K. Green, A. Fern, and J. W. Hurst, "Fast online trajectory optimization for the bipedal robot cassie," in *Robotics: Science and Systems (RSS)*, 2018.

[12] S. Seok, A. Wang, Meng Yee Chuah, D. Otten, J. Lang, and S. Kim, "Design principles for highly efficient quadrupeds and implementation on the mit cheetah robot," in *IEEE International Conference on Robotics and Automation (ICRA)*, 2013, pp. 3307–3312.

[13] B. Verrelst, R. Van Ham, B. Vanderborght, F. Daerden, D. Lefeber, and J. Vermeulen, "The pneumatic biped lucy actuated with pleated pneumatic artificial muscles," *Autonomous Robots*, vol. 18, pp. 201–213, 2005.

[14] T. Takuma, S. Hayashi, and K. Hosoda, "3d bipedal robot with tunable leg compliance mechanism for multi-modal locomotion," in *IEEE/RSJ International Conference on Intelligent Robots and Systems (IROS)*, 2008, pp. 1097 – 1102.

[15] D. Rus and M. T. Tolley, "Design, fabrication and control of soft robots," *Nature*, vol. 521, no. 7553, p. 467, 2015.

[16] E. Coevoet, A. Escande, and C. Duriez, "Soft robots locomotion and manipulation control using fem simulation and quadratic programming," in *IEEE International Conference on Soft Robotics (RoboSoft)*, 2019, pp. 739–745.

[17] R. F. Shepherd, F. Ilievski, W. Choi, S. A. Morin, A. A. Stokes, A. D. Mazzeo, X. Chen, M. Wang, and G. M. Whitesides, "Multigait soft robot," *Proceedings of the national academy of sciences*, vol. 108, no. 51, pp. 20 400–20 403, 2011.

[18] M. T. Tolley, R. F. Shepherd, B. Mosadegh, K. C. Galloway, M. Wehner, M. Karpelson, R. J. Wood, and G. M. Whitesides, "A resilient, untethered soft robot," *Soft robotics*, vol. 1, no. 3, pp. 213–223, 2014.

[19] J. M. Florez, B. Shih, Y. Bai, and J. K. Paik, "Soft pneumatic actuators for legged locomotion," in *IEEE International Conference on Robotics and Biomimetics (ROBIO)*, 2014, pp. 27–34.

[20] S. Mao, E. Dong, H. Jin, M. Xu, and K. Low, "Locomotion and gait analysis of multi-limb soft robots driven by smart actuators," in *IEEE/RSJ International Conference on Intelligent Robots and Systems (IROS)*, 2016, pp. 2438–2443.

[21] A. Sadeghi, A. Mondini, E. Del Dottore, A. K. Mishra, and B. Mazzolai, "soft-legged wheel-based robot with terrestrial locomotion abilities," *Frontiers in Robotics and AI*, vol. 3, p. 73, 2016.

[22] D. Drotman, S. Jadhav, M. Karimi, P. Dezonia, and M. T. Tolley, "3d printed soft actuators for a legged robot capable of navigating unstructured terrain," in *IEEE International Conference on Robotics and Automation (ICRA)*, 2017, pp. 5532–5538.

[23] Q. Sun, F. Gao, and X. Chen, "Towards dynamic alternating tripod trotting of a pony-sized hexapod robot for disaster rescuing based on multi-modal impedance control," *Robotica*, vol. 36, no. 7, pp. 1048–1076, 2018.

[24] C. Duriez, E. Coevoet, F. Largilliere, T. Morales-Bieze, Z. Zhang, M. Sanz-Lopez, B. Carrez, D. Marchal, O. Goury, and J. Dequidt, "Framework for online simulation of soft robots with optimization-based inverse model," in *IEEE International Conference on Simulation, Modeling, and Programming for Autonomous Robots (SIMPAR)*, 2016, pp. 111–118.

[25] J. M. Bern, P. Banzet, R. Poranne, and S. Coros, "Trajectory optimization for cable-driven soft robot locomotion," in *Robotics: Science and Systems (RSS)*, 2019.

[26] K. M. Digumarti, A. T. Conn, and J. Rossiter, "Euglenoid-inspired giant shape change for highly deformable soft robots," *IEEE Robotics and Automation Letters*, vol. 2, no. 4, pp. 2302–2307, 2017.

[27] C. Duriez, "Control of elastic soft robots based on real-time finite element method," in *IEEE International Conference on Robotics and Automation (ICRA)*, 2013, pp. 3982–3987.

[28] J. Allard, S. Cotin, F. Faure, P.-J. Bensoussan, F. Poyer, C. Duriez, H. Delingette, and L. Grisoni, "Sofa-an open source framework for medical simulation," in *Medicine Meets Virtual Reality(MMVR)*, vol. 125, 2007, pp. 13–18.

[29] E. Coevoet, T. Morales-Bieze, F. Largilliere, Z. Zhang, M. Thieffry, M. Sanz-Lopez, B. Carrez, D. Marchal, O. Goury, J. Dequidt, *et al.*, "Software toolkit for modeling, simulation, and control of soft robots," *Advanced Robotics*, vol. 31, no. 22, pp. 1208–1224, 2017.

[30] T. M. Bieze, F. Largilliere, A. Kruszewski, Z. Zhang, R. Merzouki, and C. Duriez, "Finite element method-based kinematics and closed-loop control of soft, continuum manipulators," *Soft robotics*, vol. 5, no. 3, pp. 348–364, 2018.

[31] E. Coevoet, A. Escande, and C. Duriez, "Optimization-based inverse model of soft robots with contact handling," *IEEE Robotics and Automation Letters*, vol. 2, no. 3, pp. 1413–1419, 2017.

[32] U. Saranli, M. Buehler, and D. E. Koditschek, "Rhex: A simple and highly mobile hexapod robot," *The International Journal of Robotics Research*, vol. 20, no. 7, pp. 616–631, 2001.

[33] P. Birkmeyer, K. Peterson, and R. S. Fearing, "Dash: A dynamic 16g hexapedal robot," in *IEEE/RSJ International Conference on Intelligent Robots and Systems (IROS)*, 2009, pp. 2683–2689.

[34] D. Holland, E. J. Park, P. Polygerinos, G. J. Bennett, and C. J. Walsh, "The soft robotics toolkit: Shared resources for research and design," *Soft Robotics*, vol. 1, no. 3, pp. 224–230, 2014.

[35] Y. Sugiyama, A. Shiotsu, M. Yamanaka, and S. Hirai, "Circular/-spherical robots for crawling and jumping," in *IEEE International Conference on Robotics and Automation (ICRA)*, 2005, pp. 3595–3600.